*4354–4367* *Nucleic Acids Research, 2016, Vol. 44, No. 9* *Published online 14 March 2016*
*doi: 10.1093/nar/gkw169*

# Rational design of novel N-alkyl-N capped biostable RNA nanostructures for efficient long-term inhibition of gene expression

**Montserrat Terrazas[1,*], Ivan Ivani[1], Núria Villegas[1,2], Clément Paris[3], Cándida Salvans[1], Isabelle Brun-Heath[1] and Modesto Orozco[1,2,4,*]**

[1]Institute for Research in Biomedicine (IRB Barcelona), The Barcelona Institute of Science and Technology, Joint IRB-BSC Program in Computational Biology, Baldiri Reixac 10-12, 08028 Barcelona, Spain, [2]Barcelona Supercomputing Center, Jordi Girona 29, 08034 Barcelona, Spain, [3]Department of Organic Chemistry and IBUB, University of Barcelona, Martí i Franquès 1-11, 08028 Barcelona, Spain and [4]Department of Biochemistry and Molecular Biology, University of Barcelona, 08028 Barcelona, Spain

Received November 06, 2015; Revised March 01, 2016; Accepted March 03, 2016

## ABSTRACT

**Computational techniques have been used to design a novel class of RNA architecture with expected improved resistance to nuclease degradation, while showing interference RNA activity. The *in silico* designed structure consists of a 24–29 bp duplex RNA region linked on both ends by N-alkyl-N dimeric nucleotides (BCn dimers; n = number of carbon atoms of the alkyl chain). A series of N-alkyl-N capped dumbbell-shaped structures were efficiently synthesized by double ligation of BCn-loop hairpins. The resulting BCn-loop dumbbells displayed experimentally higher biostability than their 3′-N-alkyl-N linear version, and were active against a range of mRNA targets. We studied first the effect of the alkyl chain and stem lengths on RNAi activity in a screen involving two series of dumbbell analogues targeting *Renilla* and Firefly luciferase genes. The best dumbbell design (containing BC6 loops and 29 bp) was successfully used to silence GRB7 expression in HER2+ breast cancer cells for longer periods of time than natural siRNAs and known biostable dumbbells. This BC6-loop dumbbell-shaped structure displayed greater anti-proliferative activity than natural siRNAs.**

## INTRODUCTION

RNA interference (RNAi) is an innate defense mechanism of gene regulation triggered by 21–23 nt RNA duplexes with 3′-terminal dinucleotide overhangs (siRNAs) (1,2) that are generated in the cytoplasm by Dicer cleavage of longer RNAs (3–5). After incorporation into the RISC protein complex, siRNAs induce degradation of the complementary target mRNAs. Shortly after the discovery of RNAi, synthetic siRNAs were found to produce the same effect (6,7). Since then, much effort has been made to exploit the RNAi process experimentally to inhibit the expression of genes of choice for therapeutic purposes (8,9). However, despite the attractive biomedical potential of this approach, siRNAs are not drug-like molecules. One of their most important limitations is their vulnerability to degradation by serum exo- and endonucleases (10,11).

Extensive research has been conducted to increase the biostability of these agents (8,9). These efforts have yielded a wide number of siRNAs containing chemical modifications in the sugar ring or the phosphate backbone (8,9,12–20). Relevant examples are siRNAs that incorporate electronegative substituents at the 2′-position in the sugar ring such as 2′-fluoro (12–16) and 2′-*O*-methyl substitutions (17,18), which are known to increase the biostability and thermal stabilities of siRNAs to a great extent (21–24). Another modification that has been widely studied is the phosphorothioate linkage (PS) (19,20).

Two main approaches are usually considered in order to increase nuclease resistance. The first one is based on the extensive modification of the RNA molecule. For example, Sirna Therapeutics has several products that involve combination of 2′-fluoro pyrimidines, DNA purines, PS linkages and abasic caps (9) in the sense and the guide strands. These combinations have yielded products of increased potency and long serum half-life (48–72 h) that have been successfully used in a Hepatitis B virus mouse model (25). However, the extensive modification of the siRNA molecules often is not-well tolerated by the RNAi machinery and can lead to the reduction of the gene silencing activity (7,17). The

*To whom correspondence should be addressed. Tel: +34 934020228; Fax: +34 034037175; Email: montserrat.terrazas@irbbarcelona.org
Correspondence may also be addressed to Modesto Orozco. Tel: +34 934037155; Fax: +34 034037175; Email: modesto.orozco@irbbarcelona.org

selective modification of the nuclease-sensitive sites represents an alternative approach to the extensive modification of the siRNA. For example, Alnylam Pharmaceuticals has several siRNA products that are selectively modified with 2′-*O*-methyl or 2′-fluoro substitutions at vulnerable sites (9,26) (http://www.alnylam.com/Programs-and-Pipeline/index.php). Therefore, development of minimal modification approaches aimed at improving or optimizing the properties of the siRNA molecule (e.g. by protecting the 3′-terminal ends of the duplex from exonuclease cleavage) are of significance nowadays.

With the aim of developing new and complementary approaches for modifying the siRNA molecule, in a recent study, we developed a new class of 3′-exonuclease-resistant modification (27) that involved minimal and selective alteration of the oligonucleotide. In particular, our strategy involved replacement of the 3′-terminal natural dinucleotide overhangs of siRNAs by dimeric nucleotides composed of two 2′-deoxy-5-methylcytidine units linked together by an ethyl chain through the exocyclic amino group of the nucleobase (N-ethyl-N bridged nucleosides). Based on the promising results of those studies, here we have undertaken a computational investigation of the conformational and dynamic behavior of 3′-terminal N-alkyl-N bridged nucleotides (BCn dimers; n = number of carbon atoms of the alkyl chain) that has allowed us to develop new RNA architectures with even higher nuclease resistance. In particular, dumbbell-shaped structures having a duplex RNA region comprised of 24–29 base pairs linked on both ends by BCn dimers (Figure 1).

There are only a few reports in the literature of dumbbell-shaped dsRNAs acting as siRNA precursors (28–30). Two relevant examples are nuclease-resistant RNA dumbbells with loops composed of seven natural nucleotides linked by standard phosphodiester bonds (28) and dimeric 1,2-bis(maleimido)ethane crosslinkers (29), which have been used to silence the expression of transiently transfected luciferase genes. In particular, the 7 nt-loop dumbbells were found to display significantly longer RNAi effect in cell culture than natural siRNA (28).

In view of the similarity between the BCn and 7 nt-loop dumbbells and the longer-lived RNAi activity of these structures, we decided to use them as controls in our studies. Stability studies in serum and cytosol cell extract confirmed that our BCn-loop design was more stable than the 7 nt-loop dumbbells described in the literature (28). Moreover, the best BCn-loop dumbbell design could be successfully applied to inhibit GRB7 (31) expression in HER2+ breast cancer cells and showed longer inhibitory effect than natural siRNA and their 7 nt-loop analogues (28). To our knowledge, the present work is the first example that provides data on long-term inhibition of endogenous genes induced by dumbbell-shaped RNAs.

## MATERIALS AND METHODS

### RNA synthesis

Oligonucleotide sequences that did not contain modified nucleotides were purchased from Sigma Aldrich. All modified sequences were synthesized at the 1 μmol scale via solid phase synthesis using standard phosphoramidite methods (32). Reagents for oligonucleotide synthesis including 2′-*O*-TBDMS-protected phosphoramidite monomers of $A^{Bz}$, $C^{Ac}$, $G^{dmf}$ and U, solid chemical phosphorylation reagent (5′-phosphate), the 5′-deblocking solution (3% TCA in $CH_2Cl_2$), activator solution (0.3 M 5-benzylthio-1-H-tetrazole in $CH_3CN$), CAP A solution (acetic anhydride/pyridine/THF), CAP B solution (THF/*N*-methylimidazole 84/16) and oxidizing solution (0.02 M iodine in tetrahydro-furan/pyridine/water (7:2:1)) were obtained from commercial sources.

For the synthesis of RNA strands containing BCn loops, commercially available 5′-*O*-DMT-$A^{Bz}$-3′-succinyl-LCAA-CPG, 5′-*O*-DMT-$C^{Ac}$-3′-succinyl-LCAA-CPG, 5′-*O*-DMT-$G^{dmf}$-3′-succinyl-LCAA-CPG and 5′-*O*-DMT-U-3′-succinyl-LCAA-CPG were used as the solid supports. For the synthesis of 3′-BC2-modified RNA strands, CPG functionalized with a BC2 unit (27) was used as the solid support. The coupling time was 15 min. The coupling yields of natural and modified phosphoramidites were around 95%. Incorporation of the dimeric nucleoside modification did not have a negative effect in the yield. Terminal 5′-phosphate group was incorporated by using the commercially available solid chemical phosphorylation reagent. All oligonucleotides were synthesized in DMT-OFF mode.

### Deprotection and purification of unmodified and modified RNA oligonucleotides

After the solid-phase synthesis, the solid support was transferred to a screw-cap vial and incubated at 55°C for 2 h with 1.5 ml of $NH_3$ solution (33%) and 0.5 ml of ethanol. The vial was then cooled on ice and the supernatant was transferred into a 2 ml eppendorf tube. The solid support and vial were rinsed with 50% ethanol (2 × 0.25 ml). The combined solutions were evaporated to dryness using an evaporating centrifuge. The residue that was obtained was dissolved in 1 M TBAF in THF (330 μl) and incubated at room temperature for 15 h. Then, 1 M triethylammonium acetate (TEEA) and water were added to the solution (330 μl TEEA and 330 μl water). The oligonucleotides were desalted on NAP-10 columns using water as the eluent and evaporated to dryness. The oligonucleotides were purified by 20% polyacrylamide gel electrophoresis (DMT-OFF). After purification, the RNAs were isolated by the crush and soak method, dialyzed, quantified by absorption at 260 nm and confirmed by Matrix-Assisted Laser Desorption/Ionization (MALDI) mass spectrometry (see Supplementary Table S1).

For annealing of linear siRNAs, 20 μM single strands were incubated in siRNA buffer (100 mM KOAc, 30 mM HEPES-KOH at pH 7.4, 2 mM $MgCl_2$) for 1 min at 90°C followed by 1 h at 37°C.

### Enzymatic synthesis of RNA dumbbells using T4 RNA ligase 2

Final composition of the reaction mixture (250 μl) was as follows: 2 μM 5′-phosphorylated-dsRNA, 22.5 units T4 RNA ligase 2 (New England Biolabs), 50 mM Tris-HCl (pH 7.5), 2 mM $MgCl_2$, 1 mM DTT, 400 μM ATP. After 5′-phosphorylated RNAs had been annealed, T4 RNA

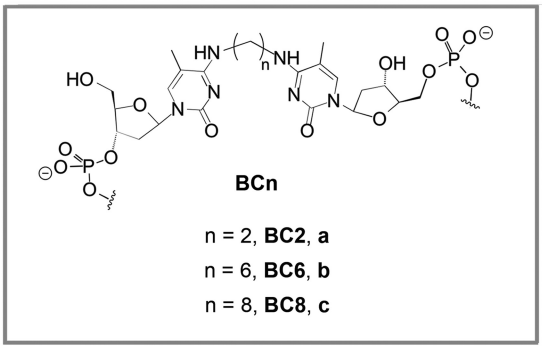


5'-AUCUGAAGAAGGAGAAAAA**BC2**-3'
3'-**BC2**UAGACUUCUUCCUCUUUUU-5' **1**

BCn(UCAAAUCUGAAGAAGGAGAAAAAAUGGUU / AGUUUAGACUUCUUCCUCUUUUUUACCAA)BCn **2a-c**

**3a-c** BCn(UCAAAUCUGAA 3' pGAAGGAGAAAAAAUGGUU 5' / AGUUUAGACUUCUUCCUCp UUUUUUACCAA 5' 3')BCn **4a-c**

G(A) G UCAAAUCUGAAGAAGGAGAAAAAAUGGUU U(C) A(A) / A C U AGUUUAGACUUCUUCCUCUUUUUUACCAA G A G **5**

5'-UCAAAUCUGAAGAAGGAGAAAAAAUGGUU-3'
3'-AGUUUAGACUUCUUCCUCUUUUUUACCAA-5' **LdsRNA29**

5'-AUCUGAAGAAGGAGAAAAATT-3'
3'-TTUAGACUUCUUCCUCUUUUU-5' **siRNA I**

3'-TTUGCACUGUGCAAGCCUCUU-5'
5'-ACGUGACACGUUCGGAGAATT-3' **scr**

**BC2**(A G U G C G C U GC 3' pU G G U G C C A A C C C U 5' / U C A C G C G A C G AC C A C G G U U G G G A)**BC2** **6**

**7a,b** BCn(AAGUGCGCUG 3' pCUGGUGCCAACCCUU 5' / UUCACGCGACGACCAC p GGUUGGGAA 5' 3')BCn **8a,b**

BCn(AAGUGCGCUGCUGGUGCCAACCCU / UUCACGCGACGACCACGGUUGGGA)BCn **9a,b**

G(A) G AAGUGCGCUGCUGGUGCCAACCCUU C(A) A(A) / A C U UUCACGCGACGACCACGGUUGGGA G A G **10**

5'-AAGUGCGCUGCUGGUGCCAACCCU**BC2**-3'
3'-**BC2**UUCACGCGACGACCACGGUUGGGA-5' **11**

5'-AAGUGCGCUGCUGGUGCCAACCCU-3'
3'-UUCACGCGACGACCACGGUUGGGA-5' **LdsRNA24**

5'-GUGCGCUGCUGGUGCCAACTT-3'
3'-TTCACGCGACGACCACGGUUG-5' **siRNA II**

**12** **BC6**(UCAAGCCCAAC 3' pAAGCUUCGAAAUGGCCAC 5' / AGUUCGGGUUGUUCGAAG p CUUUACCGGUG 5' 3')**BC6** **13**

**BC6**(UCAAGCCCAACAAGCUUCGAAAUGGCCAC / AGUUCGGGUUGUUCGAAGCUUUACCGGUG)**BC6** **14**

G(A) G UCAAGCCCAACAAGCUUCGAAAUGGCCAC U(C) A(A) / A C U AGUUCGGGUUGUUCGAAGCUUUACCGGUG G A G **15**

5'-CCCAACAAGCUUCGAAAUGTT-3'
3'-TTGGGUUGUUCGAAGCUUUAC-5' **siRNA III**

**16** **BC6**(GUGAACGAGUC 3' pCAACGUGUACGUGGUGAC 5' / CACUUGCUCAGGUUGCAC p AUGCACCACUG 5' 3')**BC6** **17**

**BC6**(GUGAACGAGUCCAACGUGUACGUGGUGAC / CACUUGCUCAGGUUGCACAUGCACCACUG)**BC6** **18**

G(A) G GUGAACGAGUCCAACGUGUACGUGGUGAC U(C) A(A) / A C U CACUUGCUCAGGUUGCACAUGCACCACUG G A G **19**

5'-CGAGUCCAACGUGUACGUGTT-3'
3'-TTGCUCAGGUUGCACAUGCAC-5' **siRNA IV**

**Figure 1.** BCn loops and RNA structures used in this study. The 29 bp RNAs **2a-c**, 24 bp RNAs **9a,b** and 29 bp RNAs **14** and **18** (and the corresponding linear controls **siRNA I**, **siRNA II**, **siRNA III** and **siRNA IV,** and 7 nt-loop dumbbell analogues **5**, **10**, **15** and **19**) target the *Renilla* and Firefly mRNAs and the 1019–1037 and 943–962 sites in the GRB7 mRNA. Top strand depicts the sense strand in the 5′→3′ direction (same as the target sequence). Bottom strand depicts the antisense strand in the 3′→5′ direction (complementary to the target). BCn: N-alkyl-N dimeric nucleoside; n: number of carbon atoms of the alkyl chain; scr: scrambled sequence; **p**: 5′-terminal phosphate group.

ligase 2 (New England Biolabs) was added to the concentrations described above and incubated at 37°C overnight. The RNA was precipitated by the addition of ethanol and sodium acetate (pH 5.2). Ligated products were purified by preparative (1 mm thick) denaturing PAGE (10%PAGE, 25% formamide, 7 M urea in 1X TBE). Bands were visualized by UV shadowing, and crushed and extracted with 0.1 M NaCl. The eluate was desalted by using Slide-A-Lyzer dyalisis columns (ThermoFischer Scientific).

### Dicer cleavage reaction of RNAs

RNAs (0.91 μM) were mixed with Dicer enzyme (0.091 units/μl; Recombinant Human Turbo Dicer Enzyme Kit from Genlantis, USA) in the buffer system supplied. The mixtures were incubated at 37°C and aliquots (2.2 μl) were taken from the mixture after 0, 1, 6 and 20 h. They were analyzed by 15% non-denaturing PAGE. The gels were visualized with SYBR Gold.

### UV-monitored thermal denaturation studies

Absorbance versus temperature curves of duplexes **LdsRNA24**, **9a**, **9b** and **10** were measured at 1 μM strand concentration in 10 mM phosphate buffer (pH 7.0) containing 1 mM EDTA. In the case of duplexes **LdsRNA29**, **2a** and **2b**, 10 mM phosphate, 5 mM EDTA buffer (pH 7.0) was used. Experiments were performed in Teflon-stoppered 1 cm path length quartz cells on a Varian-Cary-100 spectrophotometer equipped with thermoprogrammer. The samples were heated to 100°C, allowed to slowly cool to 20°C, and then warmed during the denaturation experiments at a rate of 0.5°C/min to 100°C, monitoring absorbance at 260 nm. The data were analyzed by the denaturation curve processing program, MeltWin v. 3.0. Melting temperatures ($T_m$) were determined by computerfit of the first derivative of absorbance with respect to 1/T.

### Cell culture

All cell lines (HeLa, HeLa H/P, SKBR3 and MCF7) were mantained at 37°C in a humidified atmosphere with 5% $CO_2$. HeLa and MCF7 cells were cultured in Dulbecco's modified Eagle's medium (DMEM; GIBCO) supplemented with fetal bovine serum (FBS, 10%), penicillin (100 U $ml^{-1}$) and streptomycin (100 μg $ml^{-1}$). SKBR3 cells were cultured in McCoy's modified medium (GIBCO) supplemented with FBS (10%), penicillin (100 U $ml^{-1}$) and streptomycin (100 μg $ml^{-1}$). HeLa H/P cells stably expressing pGL4.14 [luc2/Hygro] (Promega) and pRL-tk-Puro (a kind gift of Dr Alagia) were maintained under hygromycin B (200 μg $ml^{-1}$) and puromycin (2 μg $ml^{-1}$) selection pressure.

### Luciferase siRNA assays

HeLa cells were regularly passaged to mantain exponential growth. The cells were seeded one day prior to the experiment in a 24-well plate at a density of 1.5 x $10^5$ cells/well in complete DMEM containing 10% FBS (500 μl per well). Following overnight culture, the cells were treated with luciferase plasmids and siRNAs. Two luciferase plasmids—*Renilla* luciferase (pRL-TK) and firefly luciferase (pGL3) from Promega—were used as a reporter and control. Cotransfection of plasmids and siRNAs was carried out with Lipofectamine 2000 (Life Technologies) as described by the manufacturer for adherent cell lines; pGL3-control (1.0 μg), pRL-TK (0.1 μg) and siRNA duplex (20 nM) formulated into liposomes were added to each well with a final volume of 600 μl. After a 5-h incubation period, cells were rinsed once with phosphate buffered saline (PBS) and fed with 600 μl of fresh DMEM containing 10% FBS. After a total incubation period time of 22 h, the cells were harvested and lysed with passive lysis buffer (100 μl per well) according to the instructions of the Dual-Luciferase Reporter Assay System (Promega). The luciferase activities of the samples were measured with a MicroLuma*Plus* LB 96V (Berthold Technologies) with a delay time of 2 s and an integration time of 10 s. The following volumes were used: 20 μl of sample and 30 μl of each reagent (Luciferase Assay Reagent II and Stop and Glo Reagent). The inhibitory effects generated by siRNAs were expressed as normalized ratios between the activities of the reporter (*Renilla* or Firefly) luciferase gene and the control (Firefly or *Renilla*, respectively) luciferase gene.

### Statistical analysis

Data were analyzed by using the GraphPad Prism 5 program (GraphPad Software). Where appropriate, the results are expressed as mean ± standard deviation (SD). *P*-values of 0.05 or less were accepted as indicators of statistically significant data. Significant differences were assessed by Student's *t*-tests or by ANOVA to compare three or more groups followed by Bonferroni test. Each experiment was performed in triplicate.

### Analysis of GRB7 protein knockdown by Western blot

SKBR3 cells were seeded 24 h before transfection in 60 mm dishes at a density of 8 x $10^5$ cells/dish in medium containing 10% FBS. Following overnight culture, siRNA duplexes (60 nM per dish) formulated into liposomes were added to each dish with a final volume of 6 ml. Cotransfection of siRNAs was carried out using Lipofectamine 2000. After a 5-h incubation period, the transfection medium was changed to complete medium containing 10% FBS. After a 24-h, 48-h, 72-h and 6-days incubation time, the cells were harvested with PBS and lysed by incubation in RIPA buffer containing protease inhibitors (Roche) at 4°C for 1 h. Cell debris were removed by centrifugation at 8000 xg for 20 min at 4°C, and protein concentration was determined using the BCA assay (Pierce). Thirty micrograms of protein were resolved by SDS electrophoresis and transferred to a poly(vinylidene difluoride) membrane (Immobilon-P, Millipore). The membrane was blocked with 5% skim milk in TBS containing 0.1% Tween for 1 h at r.t. and subsequently probed with anti-GRB7 monoclonal rabbit antibody (Santa Cruz Biotechnology) (diluted 1:1000 in blocking buffer) overnight at 4°C. Anti-rabbit (goat) IgG HRP conjugated secondary antibody (Thermo Scientific, Rockford, IL, USA) was incubated at 1:5000 dilution in the blocking solution for 1 h at r.t. β-Actin was selected as internal control and was detected by incubation with anti-β-actin HRP conjugated antibody (Abcam) (at a dilution

of 1:20 000 in blocking buffer) for 1 h at r.t. The intensities of the bands were analyzed using ImageJ 1.45 software (Rasband, W.S., ImageJ, U. S. National Institutes of Health, Bethesda, Maryland, USA, http://imagej.nih.gov/ij/, 1997–2011).

### Cell proliferation assay

Interference with *in vitro* growth rate of SKBR3 and MCF7 cells by natural siRNAs and BC6-loop dumbbell was measured using crystal violet. 1.5 x $10^5$ SKBR3 and MCF7 cells were plated in 24-well plates. Twenty-four hours after plating (0 h) cells were transfected with control GRB7 **siRNA III**, BC6-loop dumbbell **13** and non-targeting (anti-*Renilla*) **siRNA I** (60 nM) using Lipofectamine 2000. At different time points (48 or 72 h) cells were fixed with 4% formalin for 10 min, then washed twice with distilled water and stained with 0.1% freshly prepared crystal violet for 30 min. After washing, the stain was dissolved with 10% acetic acid and subsequently quantified by absorbance at 570 nM.

### 3′-exonuclease digestions

Each RNA oligomer (120 pmol) was incubated with Phosphodiesterase I from *Crotalus adamanteus* venom (SNVPD; 340 ng, 10 mU or 680 ng, 20 mU) in a buffer containing 56 mM Tris-HCl (pH 7.9) and 4.4 mM $MgSO_4$ (total volume = 40 μl) at 37°C. At appropriate periods of time, aliquots of the reaction mixture (5 μl) were taken and added to a solution of 0.5 M EDTA, pH 8.0 (15 μl), and the mixtures were immediately frozen. The samples were analyzed by electrophoresis on 15% polyacrylamide gel under non-denaturing conditions. The oligonucleotide bands were visualized with the SYBR Gold reagent.

### Calf intestinal phosphatase-5′-exonuclease digestions

Each RNA oligomer (120 pmol) was incubated with Calf Intestinal Phosphatase (1 mU) in a buffer containing 50 mM potassium acetate, 20 mM Tris-acetate, 10 mM magnesium acetate 100 μg/ml BSA, pH 7.4 at 37°C for 30 min. The enzyme was deactivated by heating at 65°C for 10 min and the RNA products were ethanol precipitated. After resuspension with 40 μl of 100 mM sodium acetate pH 6.5 buffer, the RNA samples were treated with Bovine Spleen Phosphodiesterase (10 mU) and incubated at 37°C. At appropriate periods of time, aliquots of the reaction mixture (5 μl) were taken and added to a solution of 0.5 M EDTA pH 8.0 (15 μl), and the mixtures were immediately frozen. The samples were analyzed by electrophoresis on 15% polyacrylamide gel under non-denaturing conditions. The oligonucleotide bands were visualized with the SYBR Gold reagent.

### Stability of RNA and DNA oligonucleotides in PBS containing human serum

Each oligonucleotide (300 pmol) was incubated in PBS containing 50% of human serum (total volume = 75 μl) at 37°C. At appropriate periods of time, aliquots of the reaction mixture (5 μl) were separated and added to a solution of 0.5 M EDTA pH 8.0 (15 μl), and the mixtures were immediately frozen. The samples were run on a 15% polyacrylamide gel under non-denaturing conditions. The oligonucleotide bands were visualized with the SYBR Gold reagent.

### Stability of RNA and DNA oligonucleotides in S100 HeLa cell cytosol extract

Each oligonucleotide (100 pmol) was incubated in 20 mM HEPES-Na pH 7.9, 42 mM ammounium sulfate, 0.2 mM EDTA, 0.5 mM DTT, 20% glycerol buffer containing 10% HeLa cell cytosol extract (S100, human; Jena Bioscience) at 37°C. At appropriate periods of time, aliquots of the reaction mixture (3.7 μl) were separated and added to a solution of 0.5 M EDTA pH 8.0 (6.7 μl), and the mixtures were immediately frozen. The samples were run on a 15% polyacrylamide gel under non-denaturing conditions. The oligonucleotide bands were visualized with the SYBR Gold reagent.

### Molecular dynamics simulations

We simulated four systems, BC2-, BC6- and BC8-dumbbells (**2a**, **2b** and **2c**, respectively), as well as the linear dsRNA duplex analogue (**LdsRNA29**), used as a control system. The approach was similar to that used in previous study (27). Linker structures were first geometrically optimized using Gaussian09 (33) package from which were calculated point charges using RESP calculation (34). Simulations were done using AMBER14 package (35). We used the latest DNA force-field, parmbsc1 (36) with new RNA parameters developed recently in the lab. RNA structures were created using generic NAB module from AMBER14 package. The structures were solvated with TIP3P water molecules (37), neutralized with $Na^+$ ions (38) with an additional 0.15 M of $Na^+Cl^-$ added to the system, in order to approximate experimental conditions. Systems were minimized, annealed and equilibrated following the standard AMBER simulation protocol, with 1 ns of equilibration time. Data were analyzed using Curves+ program (39).

Molecular Dynamics (MD) simulations of the double-stranded RNA containing 3′-terminal 1,2-di(5-methylcytidin-$N^4$-yl)ethane units (**1**; Figure 1) were performed using the same approach.

## RESULTS AND DISCUSSION

### Design of N-alkyl-N capped RNA structures

We started our study by performing MD simulations of a 19 bp siRNA complementary to the 501–519 A-rich site of the *Renilla* luciferase mRNA, where each 3′-terminal dinucleotide overhang (TpT) had been replaced by a BC2 dimer (RNA **1**, Figure 1). Interestingly, starting from an intramolecular stacked conformation, the BC2 dimer progressed to a completely extended form during the course of the simulations, with the final snapshot revealing favorable stacking interactions between the nucleobase of the second subunit of the dimer and the 5′-terminal nucleobase of the complementary strand (Figure 2A), suggesting that we could take advantage of the flexibility of the dimer to create a closed dumbbell-shaped dsRNA with the 3′- and

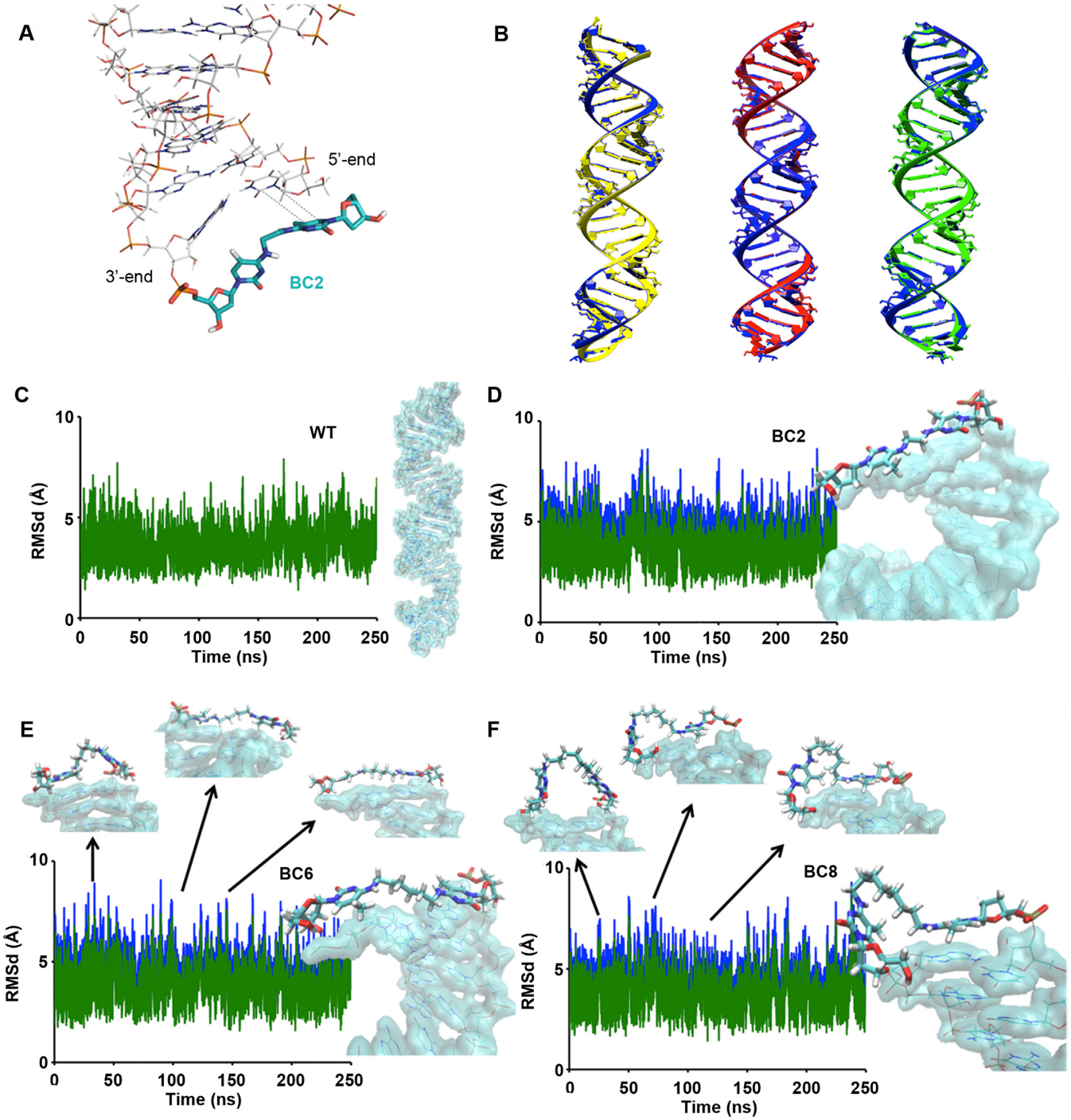


**Figure 2.** (**A**) Representative snapshot from the molecular dynamics (MD) trajectory of the RNA duplex 5′-UUUUUCUCCUUCUUCAGAU**BC2**–3′:3′-**BC2**AAAAAGAGGAAGAAGUCUA-5′ (**1**; Figure 1) showing a completely extended conformation of the BC2 dimer, with stacking interactions between its second subunit and the 5′-terminal nucleobase of the complementary strand. (**B**) Comparison of average structures of BC2- (yellow), BC6- (red) and BC8-dumbbells (green) with linear dsRNA (**LdsRNA29**; blue) from MD simulations. (**C**–**F**) RMSd plots of (**C**) linear **LdsRNA29**, (**D**) BC2-, (**E**) BC6- and (**F**) BC8-dumbbell structures with sequence 5′-AACCAUUUUUUCUCCUUCUUCAGAUUUGA-3′:3′-UUGGUAAAAAAGAGGAAGAAGUCUAAACU-5′. Representative snapshots are shown on the right side of each plot. Blue line shows RMSd evolution considering all residues, while green line shows only the linear part of the dumbbells. Linker structures are drawn with licorice representation, while the linear part is drawn in blue surface representation. Several of BC6- and BC8-dumbbell snapshots are shown to demonstrate the higher flexibility of those structures compared with BC2-linker.

5′-ends connected by a N-alkyl-N bridged nucleoside. To investigate this possibility, we proceeded to perform MD simulations of the predicted closed structure. It has been reported that the efficiency of Dicer processing increases with the length of the stem of the duplex (28). In particular, 29 bp dumbbells with loops of natural nucleotides have been found to act as better substrates for Dicer than shorter analogues. Thus, the final dumbbell-shaped structures were designed to have 29 base pairs targeting the same *Renilla* mRNA region. To identify the appropriate structural conditions needed for minimal constraints within the double-stranded RNA, three dumbbells with different alkyl chain lengths—2, 6 and 8 carbon atoms—were subjected to investigation (BC2-, BC6- and BC8-loop dumbbells **2a-c**, respectively; Figures 1 and 2B, D–F). As a control, we run MD simulations of their linear counterpart (**LdsRNA29**; Figures 1 and 2C). Interestingly, the capping of the dsRNA through BC2, BC6 and BC8 cross-linking did not alter the global geometry of the double helix. Average structures from 250 ns MD simulations (Figure 2B) revealed minimal differences in linear parts of the dumbbells compared with the control simulation (**LdsRNA29**). RMSd plots demonstrated stability of the proposed structures with neglectable effect of designed linkers on the linear part of the dumbbells (Figure 2, panels C–F). Represented snapshots in Figure 2D–F and Supplementary Figure S2 show higher flexibility of BC6- and BC8- linkers with one of its bases being stacked most of time. As expected, BC8- explored bigger conformational space taking into account its higher degrees of freedom. In the case of the BC2- linker, both of its bases kept stacking with the neighboring base-pair during the whole simulation. In terms of helical characteristics linear part of dumbbell structures are indistinguishable to its analogue counterpart, **LdsRNA29** (see Supplementary Figure S1).

### Synthesis of N-alkyl-N capped dumbbell RNAs

Encouraged by these observations, we explored the possibility of formation of these BC2-, BC6- and BC8-loop 29 bp dumbbells (**2a–c**; Figure 1). Our synthetic approach involved double ligation of a pair of hairpins with BCn loops and 5′-phosphorylated dangling ends (Figure 3A). The construction of these nanostructures began by synthesizing the BCn-loop dimeric nucleosides according to methods described previously (see the Supporting Information) (27,40). The resulting dimers were converted to the desired phosphoramidites (Scheme S1), which were incorporated into the BCn-loop internal position of a set of pairs of hairpins (pairs **3a-c**:**4a-c**; Figure 3A) by using an automated DNA/RNA synthesizer and 2′-*O*-TBDMS-protected phosphoramidites of natural ribonucleotides.

Each pair of hairpins (**3a:4a**, **3b:4b** and **3c:4c**) was incubated with T4 RNA ligase 2. Analysis of the reactions of the BC2- and BC6-loop pairs (**3a:4a** and **3b:4b**) by PAGE suggested the formation of the desired closed structures (dumbbells **2a** and **2b**, respectively; Figure 3B) as major products. In both cases, we observed the formation of a new band that migrated more slowly than the starting hairpins. 5′- and 3′-exonuclease assays (Figure 3C and D) confirmed the desired double-ligated closed structure of these RNAs. After isolation (by PAGE) and incubation with the 3′-exonuclease snake venom phosphodiesterase I (SNVPD), both products of ligation (**2a** and **2b**) remained untouched after 2 days of incubation (Figure 3D). The same occurred when they were treated with calf intestinal phosphatase (CIAP) and 5′-exonuclease bovine spleen phosphodiesterase (BSP) (Figure 3C). In contrast to this, pre-ligated hairpins **3a** and **4a** and a synthetic BC2-dumbbell-shaped RNA with an internal nick (**6**; Figure 1; that had been prepared as a control) were hydrolyzed in the presence of BSP and SNVPD (Figure 3C and D). In the case of the ligation of the hairpins containing a more flexible loop (**3c** and **4c**; BC8 loop), we observed the formation of a major product of much lower mobility than the products of the former ligations (**2a** and **2b**) and an almost undetectable band of similar mobility to that of the BC2 and BC6-loop dumbbells **2a** and **2b** (Figure 3B), which could not be isolated. After isolation of the product of lower mobility (major product) treatment with CIAP–BSP and SNVPD led to rapid hydrolysis, (Figure 3C and D), confirming its nicked structure. Taken together, these results suggest that the processes of hairpin formation and ligation are less favorable in the cases of RNAs having more flexible loops (BC8), which could be explained by the lower degree of BC loop-RNA nucleobase stacking predicted by our calculations for the final BC8-loop structure.

Having established conditions for dumbbell formation, we applied them to the synthesis of a second group of dumbbells. With the aim of comparing our dumbbell design with a known biostable dumbbell-shaped RNA (28), we focused on the synthesis of BC2- and BC6-loop versions of an anti-Firefly mRNA 24 bp dumbbell with loops of natural nucleotides (**10**, Figure 1) described in the literature (dumbbells **9a,b**; Figures 1 and 3A). In this case, the reactions of ligation of the corresponding pairs of hairpins (**7a**:**8a** and **7b**:**8b**; BC2- and BC6-loops, respectively) proceeded with high efficiency to give the desired closed structures (**9a,b**; Figure 3B), which were confirmed by the 5′-exo- and 3′-exonuclease assays (Figure 3C and D). This can be attributed to the higher G:C content of this sequence, which might favor the process of formation of the hairpins, due to their higher thermal stability.

### Stability of RNA dumbbells and linear controls in human serum and cell extracts

To determine their biological stability, the BCn-loop dumbbells and their corresponding linear siRNA and nicked controls were incubated in 50% human serum at 37°C. To compare them with known nuclease-resistant dumbbell structures, the serum stability of the 7 nt-loop version of dumbbells **9a,b** [**10** (Figure 1 and Supplementary Figure S3), which was synthesized according to the literature (28)] was also evaluated. Figure 4 shows the degradation profile of the most representative examples: the BC2- and BC6-dumbbells **9a** and **9b**, their siRNA, 1-nicked and 7 nt-loop versions (**siRNAII**, **6** and **10**, respectively) and the 3′-BC2 modified linear analogue **11** (Figure 1), which was synthesized as a control. Unmodified **siRNA II** displayed very low stability. Complete degradation was observed in only 4 h. The 1-nicked analogue **8** was hydrolyzed even faster. Interestingly, the BC-loop structures displayed strongly enhanced stability. The integrated intensities of the gel bands

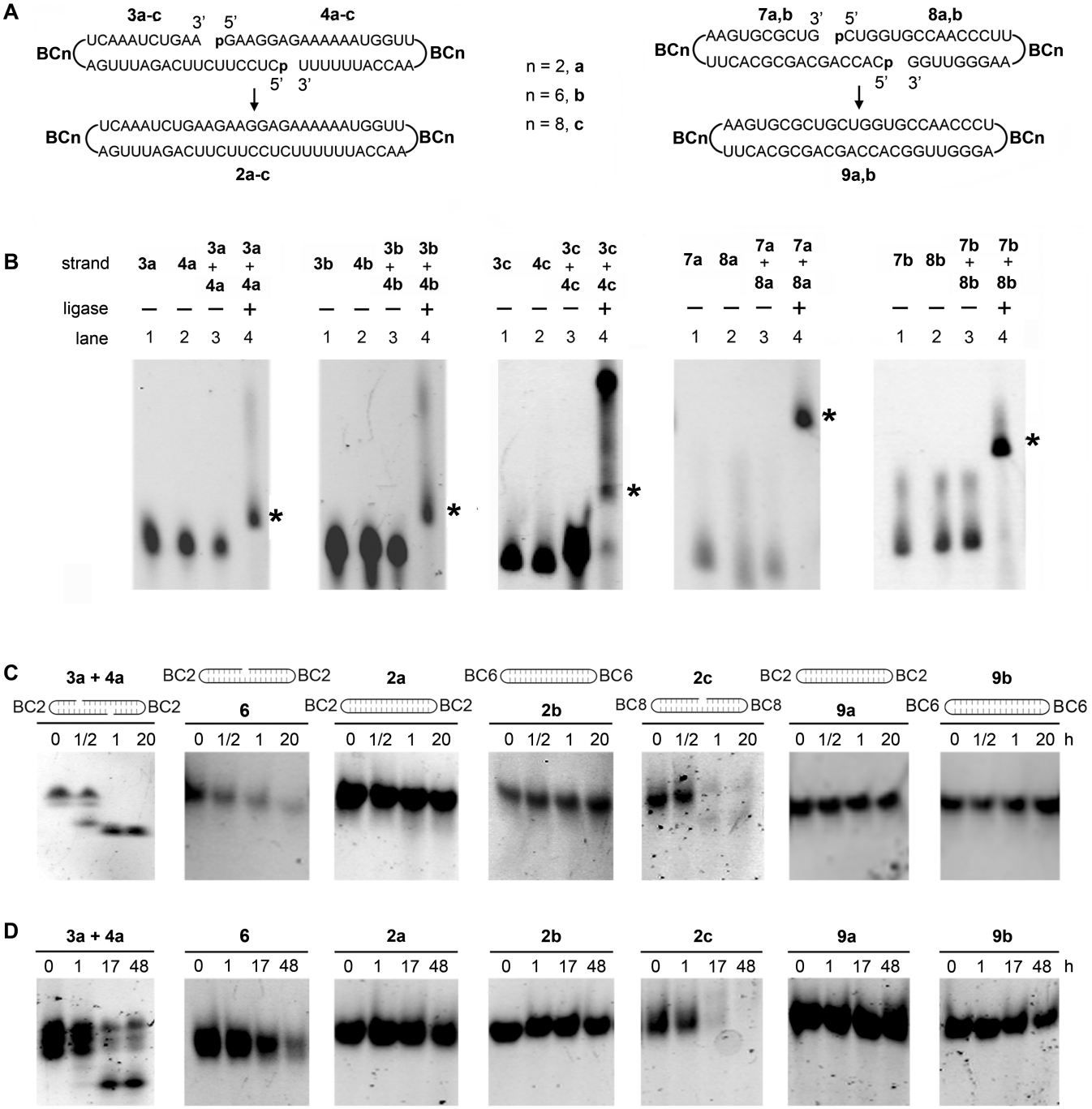


**Figure 3.** (**A**) Reaction of formation of the two sets of luciferase dumbbells used in our studies [targeting *Renilla* (**2a-c**) and Firefly (**9a,b**) mRNAs]. (**B**) Analysis of the ligation reactions by denaturing 15% PAGE containing 25% formamide and 7 M urea in 1X TBE. * means double-ligated dumbbell-shaped structure. (**C** and **D**) Incubation of RNAs with (C) calf intestinal phosphatase and bovine spleen phosphodiesterase and (D) snake venom phosphodiesterase I (SNVPD). Analysis of the exonuclease digestions by 15% non-denaturing PAGE. All oligonucleotides were withdrawn at indicated points, separated and visualized with SYBR Gold.

showed that ∼35% and 5% of the BC2-loop dumbbell **9a** remained untouched after 24 and 48 h of incubation, respectively. Its BC6-loop analogue (**9b**) displayed similar stability, with 40% and 5% of intact RNA after 24 and 48 h. In contrast, its 7 nt-loop dumbbell version (**10**) and the 3′-BC2-modified dsRNA **11** were degraded in 12 and 24 h, respectively.

To confirm that the BCn-loops also protect the RNA from nuclease degradation in complex cellular mixtures, we studied the degradation of RNAs **siRNA II**, **6**, **9a**, **9b**, **10** and **11** in 10% S100 cytosolic extract from HeLa cells (Supplementary Figure S4) (41). As observed with human serum (Figure 4), the BCn-loop-modified dumbbells (**9a** and **9b**) were significantly more stable than the corresponding 3′-

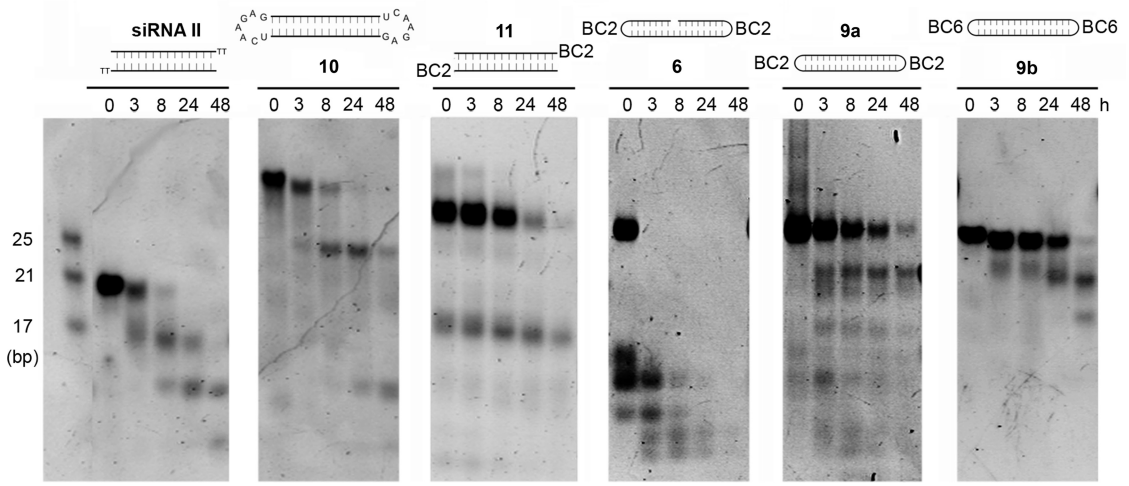


**Figure 4.** 15% non-denaturing polyacrylamide gels of unmodified **siRNA II**, 7 nt-loop dumbbell **10**, 3′-BC2-modified linear dsRNA **11**, 1-nicked structure **6**, BC2-loop and BC6-loop dumbbells **9a** and **9b** (respectively) incubated in phosphate buffered saline (PBS) containing 50% human serum at 37°C. All oligonucleotides were withdrawn at indicated points, separated by 15% native PAGE and visualized with SYBR Gold.

BC2-modified linear analogue and even higher than their 7 nt-loop version (**10**).

### Thermal denaturation and circular dichroism studies

Connection of the ends of the duplex through a BC loop gave a great increase in thermal stability (Supplementary Figure S5). The melting temperatures ($T_m$) of the 24 bp BC2- and BC6-loop dumbbells **9a** and **9b** were >25°C higher than that of their linear counterpart (**LdsRNA24**) (>95°C for **9a,b** versus 73°C for **LdsRNA24**) and slightly higher than that of their 7 nt-loop analogue **10** (∼95°C; Supplementary Figure S5A). Similar results were obtained for the second group of 29 bp structures ($T_m$s of 79°C and 77°C for BC2- and BC6-dumbbells **2a** and **2b**, versus 54°C for **LdsRNA29**; Supplementary Figure S5B). Moreover, CD analysis confirmed that the siRNA BC2- and BC6- capping does not alter the structure of the double-helix. The CD spectra of all the synthesized dumbbells superimposed well to those of their siRNA analogues (Supplementary Figure S6), confirming an A-type RNA-like structure.

### RNA recognition and cleavage by Dicer

Dicer is a RNase III-like multi-domain protein composed of a DExH/DEAH RNA helicase domain, a PAZ signature, two neighboring RNAse III-like domains and a dsRNA-binding domain (3–5,42). The helicase domain promotes translocation of the enzyme along the dsRNA and structural rearrangement of the substrate required for cleavage, whereas PAZ binds to the 2 nt 3′ overhang of its dsRNA substrate (43). It has been proposed that canonical Dicers preferentially cleave dsRNAs possessing free termini, by measuring from the 3′-end (bound to the PAZ domain) to the RNase III active site (4). However, despite the absence of free RNA ends in capped structures, dumbbell RNAs can be processed by Dicer (28,29,44). The similarity of the dumbbell stem with a canonical A-like RNA duplex found in our MD simulation suggest also that our constructs should be substrates of Dicer.

In order to investigate the effect of the N-alkyl-N dimeric nucleotides on Dicer recognition, all the synthesized BC-dumbbells were incubated with recombinant human Dicer and subjected to native gel electrophoresis. As shown in Figure 5, all the dumbbells were indeed recognized and digested by the enzyme. In the case of the shorter dumbbells (24 bp; **9a** and **9b**), RNAs shorter than 20 bp were obtained as the major products. Under the same conditions, the longer dumbbell **2b** (29 bp; BC6-loop) was digested almost completely to sequences of about 21 bp, which is in accordance with length of the Dicer products of long dsRNAs (3–5), whereas the less flexible 29 bp BC2-loop analogue **2a** was slowly digested to a mixture of shorter products. As expected (3), the treatment did not change **siRNA I**.

The above described results suggest that Dicer recognizes this class of capped dsRNAs and that a decrease in the lengths of the stem and the alkyl chain increases the degree of resistance to Dicer cleavage, leading to longer digestion times and shorter products. This could be attributed to steric effects caused by the terminal loops over the Dicer active site and to the lower flexibility of N-alkyl-N caps possessing short alkyl chains (see Figure 2D–F). Steric contacts between the loop and Dicer residues might force the enzyme to bind to internal regions located far away from the loops, which would lead to short processing products in the case of shorter duplexes. On the other hand, the higher flexibility predicted for the longer alkyl linkers might favor the structural rearrangements (helicase-promoted) involved in the digestion process.

### RNAi activities of BCn-loop dumbbells targeting *Renilla* and Firefly mRNAs

To investigate if our dumbbell designs can be processed by Dicer not only *in vitro*, but also *in vivo*, we carried out two parallel experiments with the two groups of BCn-loop dumbbells [targeting *Renilla* (**2a,b**) and Firefly (**9a,b**) luciferases], with their corresponding siRNA controls [**siRNA I** and **siRNA II** (Figure 1) as controls for dumbbells **2a,b**

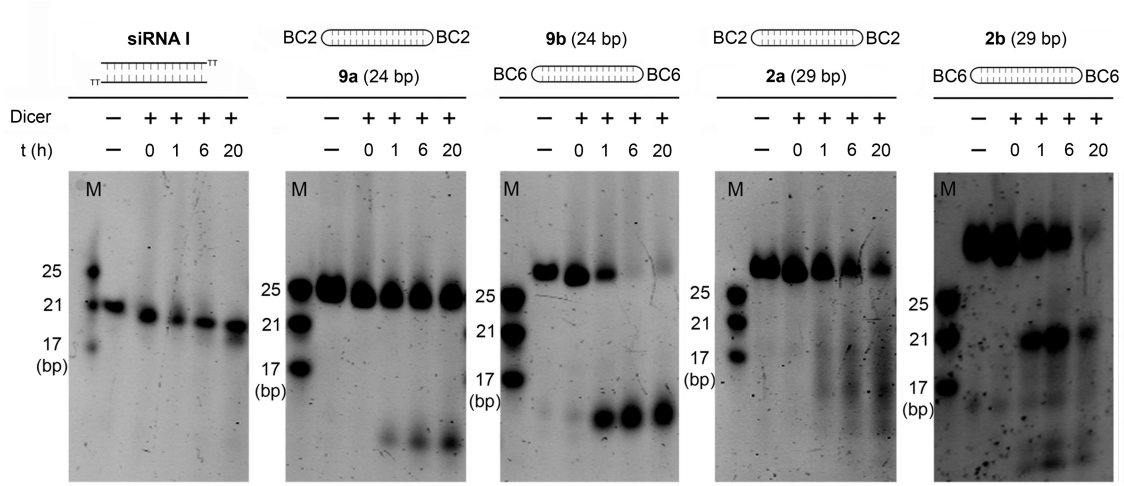


**Figure 5.** Analysis of the Dicer cleavage reaction of RNA dumbbells. Annealed RNAs were incubated with recombinant human Dicer at 37°C, and aliquots were withdrawn at 0, 1, 6 and 20 h. The reaction mixtures were analyzed by 15% native PAGE and visualized with SYBR Gold.

and **9a,b**, respectively], their 7 nt-loop dumbbell analogues [29 bp anti-*Renilla* dumbbell **5** and 24 bp anti-Firefly dumbbell **10**; Figure 1 and Supplementary Figure S3; synthesized by double ligation of 5′-phosphorylated dsRNAs, according to the literature (28)] and with a non-targeting siRNA (**scr**; Figure 1). HeLa cells were co-transfected with the dual reporter plasmids pRL-TK and pGL3 and with the various RNAs (20 nM), and the expression levels of the two luciferase genes were measured 24 h after transfection (Figure 6; panels A and B). Remarkably, all the dumbbells displayed significant target reduction. By comparing *Renilla* and Firefly dumbbells **2a,b** (Figure 6A) and **9a,b** (Figure 6B) with their corresponding siRNA controls [**siRNA I** (Figure 6A) and **siRNA II** (Figure 6B), respectively], we observed that a BC6 loop is better tolerated than the shorter BC2 loop. On the other hand, comparing RNAs **9a,b** (Figure 6B) with **2a,b**, (Figure 6A) and RNA **10** with **5**, we inferred that as the stem length increased (from 24 to 29 bp, respectively), the inhibitory effect (with respect to their unmodified siRNA analogues) significantly improved. Finally, by comparing BC2- and BC6-loop RNAs with their corresponding 7 nt-loop analogues, we observed that the activities of 7 nt-loop dumbbells are higher than that of the BC2-loop RNAs and slightly lower than that of their BC6-loop counterparts. [(98 ± 0.5)%, (78 ± 1.5)%, (91 ± 0.5)% and (88 ± 0.5)% gene knockwdown for the 24 bp RNAs **siRNA II**, **9a**, **9b** and **10**, respectively (Figure 6B), and (88 ± 2)%, (80 ± 0.5)%, (84 ± 1.5)% and (82 ± 0.5)% gene knockwdown for the 29 bp RNAs **siRNA I**, **2a, 2b** and **5** (Figure 6A)]. The most promising design corresponded to the 29 bp BC6-loop dumbbell **2b** (Figure 6A). Although it showed suppression levels slightly lower than that of its siRNA control [(84 ± 1.5)% for **2b** versus (88 ± 2)% for **siRNA I;** Figure 6A], a time-course experiment revealed that it had prolonged activity. The 7 nt-loop dumbbell analogue **5** also had RNAi effect longer than **siRNA I**, but the lifetime of its activity was lower than that of BC6-loop dumbbell **2b**. In a different experiment, HeLa H/P cells stably overexpressing the *Renilla* and Firefly vectors were transfected with **2b**, **5** and **siRNA I** (25 nM), and the RNAi activities of the three RNAs were compared over a period of 6 days (Figure 6C). Very interestingly, on day 6, the suppression activity of the BC6-dumbbell **2b** was significantly higher than that of RNAs **siRNA I** and **5** (7 nt-loop analogue)[(45 ± 1.5%) gene knockdown for **2b** versus (24 ± 2%) and (34 ± 1)% for **siRNA I** and **5**, respectively, $P < 0.0001$ and $P < 0.001$; Supplementary Figure S8].

Taken together, the results obtained from our RNAi experiments *in vivo* are in good agreement with the digestion pattern observed for *in vitro* Dicer cleavage (Figure 5), suggesting that capping the ends of the duplex with BCn loops leads to a slow release of the functional RNAs, permitting longer and then more effective RNAi effect. Our time-course experiments suggest that the presence of 7 nt-loops connecting the ends of the duplex causes a similar effect, although significantly smaller than that observed in the case of the BC6 loop.

### Gene silencing activity of dumbbell RNA targeting GRB7

To further determine the scope of application of our nanostructures, we decided to target an endogenous therapeutically relevant gene. We focused on GRB7 because of its important role in breast cancer biology and its supposed role in anti-cancer drug resistance (31,45–48). GRB7 is an adaptor protein involved in receptor tyrosine kinase signaling which has a key role in HER2 signaling, promoting cell survival and migration (31). It has been reported that expression of GRB7 in the HER2 overexpressed breast cancer subtype contributes to the aggressive nature of the tumor (45) and that HER2 signaling inhibition causes GRB7 upregulation. Moreover, it has also been demonstrated that knockdown of GRB7 by RNA interference potentiates the activity of HER2-targeting drugs (47), leading to decreases in cell proliferation (45).

The most promising dumbbell design, (29 bp stem and a BC6 loop), was used to synthesize a dumbbell targeting the 1019–1037 site of the GRB7 mRNA (GenBank code: BC006535.2), using a previously described sequence (dumbbell **14**, Figure 1 and Figures S3 and S7) (49). For comparison purposes, the corresponding 7 nt-loop ana-

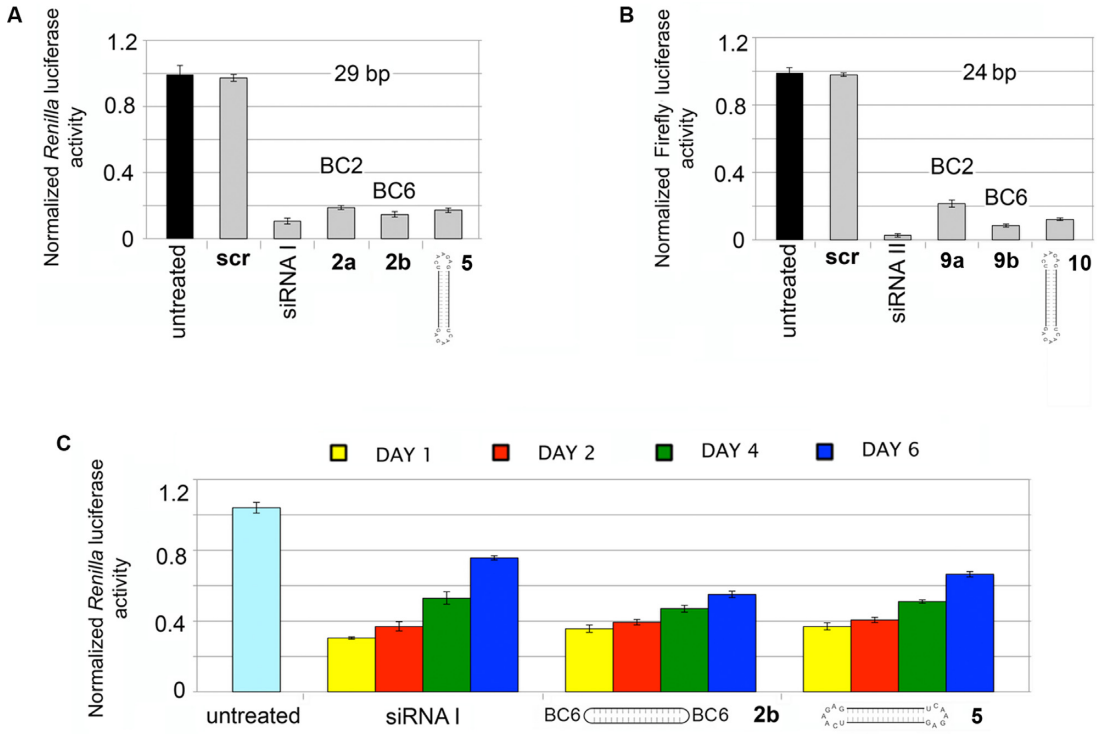


**Figure 6.** (**A** and **B**) Plots of specific activity for BCn- and 7 nt-loop dumbbells and unmodified siRNAs targeting the *Renilla* (**2a,b**, **5** and **siRNA I**; panel A) and the Firefly (**9a,b**, **10** and **siRNA II**; panel B) luciferase mRNAs in HeLa cells. Cells were co-transfected with the dual reporter plasmids pRL-TK and pGL3 and with the various RNAs, and the expression levels of the two luciferase genes were measured 24 h after transfection. Untreated cells: cells treated with plasmids alone. (**C**) Time-course experiments with BC6-dumbbell **2b**, 7 nt-loop dumbbell **5** and **siRNA I** targeting *Renilla* luciferase in HeLa H/P cells stably overexpressing the *Renilla* and Firefly vectors. Untreated cells: cells treated with the transfection agent alone. In all cases, bars indicate standard deviation.

logue (**15**) was also prepared [according to the literature (28); Supplementary Figure S3]. Transfection with the non-targeting control **siRNA I** (anti-*Renilla* luciferase siRNA) served as a negative control. Levels of GRB7 protein after treating the HER2+ breast cancer cell line SKBR3 with anti-GRB7 BC6- and 7 nt-loop dumbbells **14** and **15** and with a known anti-GRB7 siRNA as positive control (**siRNA III**; Figure 1) are shown in Figure 7A. In the three cases (**siRNA III** and dumbbells **14** and **15**), the inhibition of GRB7 protein expression was very small on day 1, whereas after 48 h, the GRB7 expression was reduced by 95%, 92% and 78% in the cases of **siRNA III** and dumbbells **14** and **15**, respectively. Very interestingly, the inhibitory effect of the BC6-loop dumbbell **14** was marked at 72 h and persisted up to 6 days, whereas unmodified **siRNA III**, starts losing efficiency after 72 h. Although the activity of the 7 nt-loop dumbbell **15** was also marked at 72 h (100% GRB7 suppression), it also started to decrease at this point, although significantly slower than unmodified **siRNA III**. On day 6, the suppression activity of the BC6-loop dumbbell **14** was 1.6-fold and 3.8-fold more potent than those of RNAs **15** (7 nt loop) and **siRNA III**, respectively, with cells treated with dumbbell **14** showing a marginal 5% expression of GRB7.

These results were further confirmed using a different siRNA sequence that had as target the 943–961 site of the same mRNA (GRB7) (GenBank code: BC006535.2) (45). The BC6-loop dumbbell directed against this second region (**18**; Figure 1; synthesized by double ligation of BC6-loop hairpins **16** and **17**; Supplementary Figure S7) induced changes in gene expression profiles over the time-course similar to the ones observed for anti-GRB7 BC6-loop dumbbell used in our first series of studies (**14**, see panels A and B in Figure 7). As observed in the first case (dumbbell **14**; Figure 7, panel A), on day 6, this second BC6-loop dumbbell construct (**18**) displayed RNAi activity significantly higher than its corresponding 7 nt-loop analogue [**19**; which was also synthesized (28), for comparison purposes (Supplementary Figure S3)] and much higher than the corresponding unmodified siRNA of the same sequence (**siRNA IV**), which was used as positive control (5% of GRB7 expression for BC6-loop dumbbell **18** versus 15% and 68% for 7 nt-loop dumbbell **19** and unmodified **siRNA IV**, respectively). In contrast to what had been observed for the first series of anti-GRB7 dumbbells (**14** and **15**), both dumbbells **18** and **19** presented their maximum activity at 48 h. BC6-dumbbell remained still completely active at 72 h, whereas the 7 nt-loop analogue **15** underwent a slight decrease in activity at this point (95% and 100% GRB7 suppression at time points 72 and 48 h, respectively). This difference in the delay of activity observed for the two sets of anti-GRB7 dumbbells could be attributed to possible sequence-dependent effects on Dicer cleavage (50,51), which might influence in the rate of processing and release of the active RNA species.

Taken together, our results suggest that the longer-lived RNAi activity observed for the BC6-loop dumbbell design

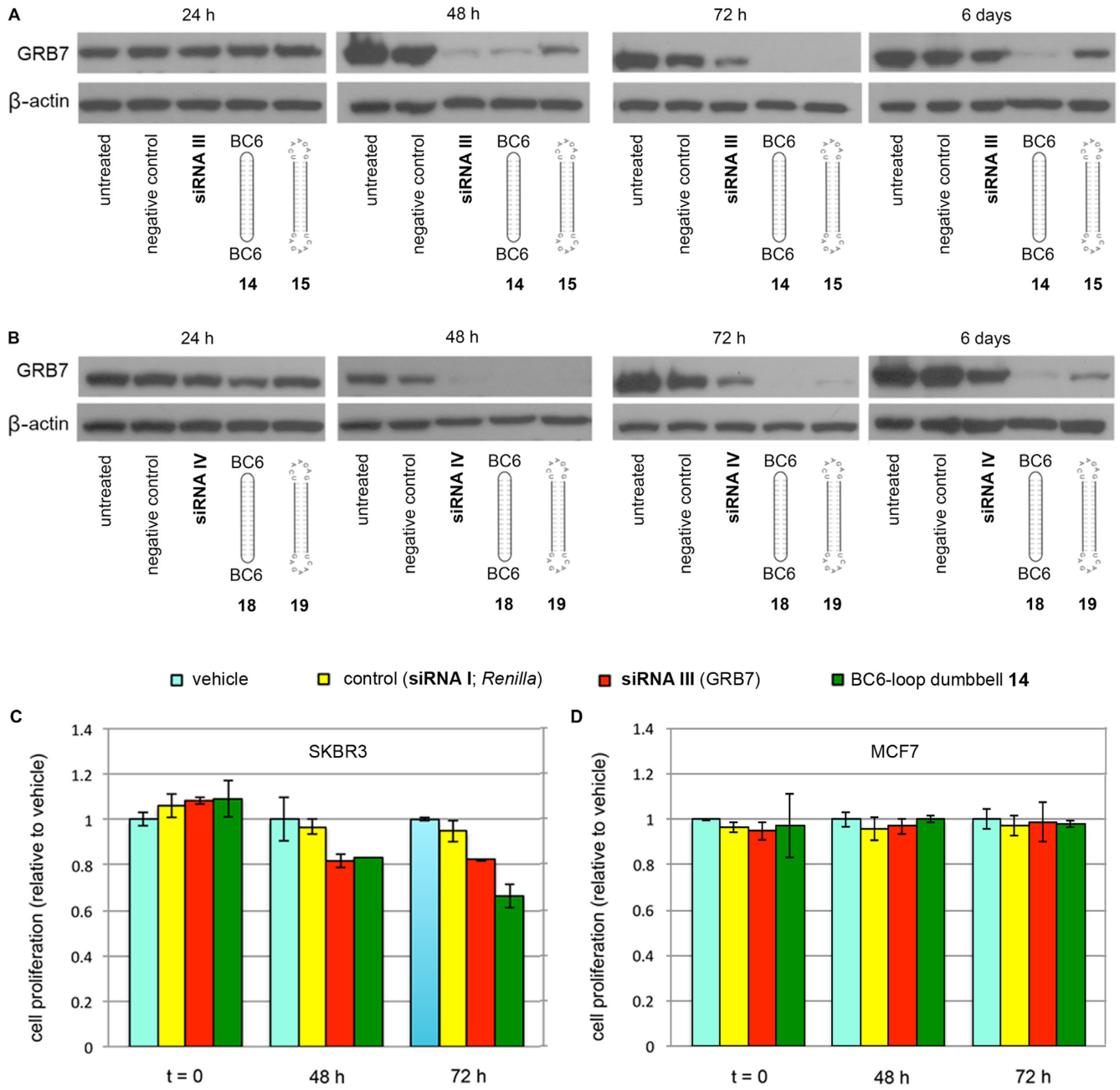


**Figure 7.** (**A** and **B**) Representative immunoblots for GRB7 and β-actin (internal control) from SKBR3 cells treated with (A) BC6-dumbbell **14**, 7 nt-loop dumbbell **15** and **siRNA III** targeting the 1019–1037 site of GRB7 mRNA and with (B) BC6-dumbbell **18**, 7 nt-loop dumbbell **19** and **siRNA IV** targeting the 943–961 site of GRB7 mRNA. In both cases (A and B) non-targeting **siRNA I** (60 nM) was used as negative control. (**C** and **D**) Proliferation assay after transfection with BC6-dumbbell **14**, **siRNA III** targeting the GRB7 mRNA and non-targeting control **siRNA I** (60 nM). The growth of (C) SKBR3 and (D) MCF7 cells were assessed using crystal violet assay and plotted as a percentage of proliferation relative to the vehicle control cells.

is due to the unique BCn-loop modification connecting the ends of the RNA duplex. Although a standard dumbbell RNA design (7 nt-loop; **15** and **19**) confers greater duration of action than a wt-siRNA, (see Figures 6C, 7A and B), our results demonstrate that the BCn-loop design leads to even longer-lived activity.

Finally, we evaluated the effect of dumbbell-mediated GRB7 knockdown on cell proliferation, quantified on 48 and 72 h after RNA transfection using the crystal violet cell viability assays in SKBR3 cells. Viability assays in cells transfected with anti-GRB7 **siRNA III** and dumbbell **14** (targeting the 1019–1037 site) and with the negative (non-targeting) control **siRNA I** (Figure 7C) revealed that 72 h after transfection, proliferation was significantly lower in **14**-transfected cells compared with unmodified **siRNA III**-transfected cells [(66 ± 5)% cell proliferation for **14** versus (82 ± 1)% for **siRNA III**; $P < 0.05$; Supplementary Figure S9]. On the contrary, MCF7 cells, that

do not have HER2 and GRB7 amplification, and express very low levels of GRB7, were unaffected when treated under the same conditions (Figure 7D). Very similar effects were observed when we used the second group of anti-GRB7 RNAs (**siRNA IV**, **18** and **19**; targeting the 943–961 site; see Supplementary Figure S10). In all cases, the dumbbell structures displayed higher anti-proliferative activity than natural siRNAs. In summary, BC6-loop dumbbell structures have excellent long-term inhibitory properties of the synthesis of GRB7—probably related to their higher biostability—which is translated in an excellent antiproliferation profile.

## CONCLUSIONS

In summary, computational studies on dsRNAs containing 3′-terminal bridged N-alkyl-N dimeric nucleotides (BC dimers) have allowed us to design new dumbbell-shaped BC-loop RNA architectures with higher biostability than their linear 3′-BC-modified version and the 7 nt-loop dumbbells described in the literature. The best dumbbell design, corresponding to a BC-loop dimer with a 6 carbon atoms alkyl linker and a stem length of 29 bp, could be used for targeting the relevant GRB7 oncogene in SKBR3 breast cancer cells with longer duration of action and higher antiproliferative effects than an unmodified siRNA. This class of alteration represents a complementary siRNA modification approach that might offer an avenue for the development of new potentially active derivatives. As the BC-loop N-alkyl-N bridged nucleosides have two free hydroxyl groups, they could participate in the conjugation with other biomolecules acting as delivery systems. The study of these and other potential biomedical applications are currently underway in our laboratory. Moreover, as our modification is located at the ends of the RNA duplex, it could be used in combination with conventional siRNA chemistries at selected internal positions (51) to optimize the properties of the siRNA molecule, giving rise to therapeutic RNAs with even higher nuclease resistance.

## SUPPLEMENTARY DATA

Supplementary Data are available at NAR Online.

## ACKNOWLEDGEMENTS

The HeLa H/P cell line was kindly provided by Dr A. Alagia (IQAC, CSIC, Barcelona, Spain). We thank Dr M. Soler-López, Dr. M. Royo, Prof. Dr R. Eritja, Prof. Dr E. Pedroso, Prof. Dr A. Grandas, Dr A. Aviñó, A. Fàbregas and Dr I. Faustino for their help and valuable comments. IRB Barcelona is the recipient of a Severo Ochoa Award of Excellence from MINECO (Government of Spain). All the experimental work was performed in the EBL laboratory.

## FUNDING

Instituto de Salud Carlos III [Miguel Servet Program, CP13/00211, 205024141 to M.T.]; Spanish MINECO [BIO2012–32869 and BIO2015-64802-R to M.O.]; AGAUR (to M.O.); ERC Council (SimDNA, grant 291433, to M.O.). M.O. is an ICREA Academia fellow. Funding for open access charge: ERC Council [grant 291433 (simDNA)].

*Conflict of interest statement.* None declared.

## REFERENCES

1. Fire,A., Xu,S., Montgomery,M.K., Kostas,S.A., Driver,S.E. and Mello,C.C. (1998) Potent and specific genetic interference by double-stranded RNA in Caenorhabditis elegans. *Nature*, **391**, 806–811.
2. Elbashir,S.M., Harborth,J., Lendeckel,W., Yalcin,A., Weber,K. and Tuschl,T. (2001) Duplexes of 21-nucleotide RNAs mediate RNA interference in cultured mammalian cells. *Nature*, **411**, 494–498.
3. Kim,D.-H., Behlke,M.A., Rose,S.D., Chang,M.-S., Choi,S. and Rossi,J.J. (2005) Synthetic dsRNA Dicer substrates enhance RNAi potency and efficacy. *Nat. Biotechnol.*, **23**, 222–226.
4. MacRae,I.J., Zhou,K.H., Li,F., Repic,A., Brooks,A.N., Cande,W.Z., Adams,P.D. and Doudna,J.A. (2006) Structural basis for double-stranded RNA processing by Dicer. *Science*, **311**, 195–198.
5. Park,J.E., Heo,I., Tian,Y., Simanshu,D.K., Chang,H., Jee,D., Patel,D.J. and Kim,V.N. (2011) Dicer recognizes the 5′ end of RNA for efficient and accurate processing. *Nature*, **475**, 201–205.
6. Elbashir,S.M., Lendeckel,W. and Tuschl,T. (2001) RNA interference is mediated by 21- and 22-nucleotide RNAs. *Genes Dev.*, **15**, 188–200.
7. Elbashir,S.M., Martinez,J., Patkaniowska,A., Lendeckel,W. and Tuschl,T. (2001) Functional anatomy of siRNAs for mediating efficient RNAi in Drosophila melanogaster embryo lysate. *EMBO J.*, **20**, 6877–6888.
8. Deleavey,G. and Damha,M.J. (2012) Designing chemically modified oligonucleotides for targeted gene silencing. *Chem. Biol.*, **19**, 937–954.
9. Watts,J.K., Deleavey,M.J. and Damha,M.J. (2008) Chemically modified siRNA: tools and applications. *Drug Discov.Today*, **13**, 842–855.
10. Choung,S., Kim,Y.J., Kim,S., Park,H.-O. and Choi,Y.-C. (2006) Chemical modification of siRNAs to improve serum stability without loss of efficacy. *Biochem. Biophys. Res. Commun.*, **342**, 919–927.
11. Shaw,J.-P., Kent,K., Bird,J., Fishback,J. and Froehler,B. (1991) Modified deoxyoligonucleotides stable to exonuclease degradation in serum. *Nucleic Acids Res.*, **19**, 747–750.
12. Harborth,J., Elbashir,S.M., Vanderburgh,K., Manninga,H., Scaringe,S.A., Weber,K. and Tuschl,T. (2003) Sequence, chemical, and structural variation of small interfering RNAs and short hairpin RNAs and the effect on mammalian gene silencing. *Antisense Nucleic Acid Drug Dev.* **13**, 83–105.
13. Wilds,C.J. and Damha,M.J. (2000) 2′-Deoxy-2′-fluoro-β-D-arabinonucleosides and oligonucleotides (2′F-ANA): synthesis and physicochemical studies. *Nucleic Acids Res.*, **28**, 3625–3635.
14. Deleavey,G.F., Watts,J.K., Alain,T., Robert,F., Kalota,A., Aishwarya,V., Pelletier,J., Gewirtz,A.M., Sonenberg,N. and Damha,M.J. (2010) Synergistic effects between analogs of DNA and RNA improve the potency of siRNA-mediated gene silencing. *Nucleic Acids Res.*, **38**, 4547–4557.
15. Chiu,Y.L. and Rana,T.M. (2003) siRNA function in RNAi: A chemical modification analysis. *RNA*, **9**, 1034–1048.
16. Braasch,D.A., Jensen,S., Liu,Y., Kaur,K., Arar,K, White,M.A. and Corey,D.R. (2003) RNA interference in mammalian cells by chemically-modified RNA. *Biochemistry*, **42**, 7967–7975.
17. Czauderna,F., Fechtner,M., Dames,S., Aygün,H., Klippel,A., Pronk,G.J., Giese,K. and Kaufmann,J. (2003) Structural variations and stabilising modifications of synthetic siRNAs in mammalian cells. *Nucleic Acids Res.*, **31**, 2705–2716.
18. Amarzguioui,M., Holen,T., Babaie,E. and Prydz,H. (2003) Tolerance for mutations and chemical modifications in a siRNA. *Nucleic Acids Res.* **31**, 589–595.
19. Eckstein,F. (1985) Nucleoside phosphorothioates. *Annu. Rev. Biochem.*, **54**, 367–402.
20. Eckstein,F. (2000) Phosphorothioate oligodeoxynucleotides: what is their origin and what is unique about them? *Antisense Nucleic Acid Drug Dev.*, **10**, 117–121.
21. Viazovkina,E., Mangos,M.M., Elzagheid,M.I. and Damha,M.J. (2002) Synthesis of 2'-fluoroarabinonucleoside phosphoramidites and their use in the synthesis of 2'F-ANA. *Curr. Prot. Nucleic Acid Chem.* John Wiley & Sons, Vol. **4.15**, pp. 1–22.

22. Watts,J.K. and Damha,M.J. (2008) 2′F-Arabinonucleic acids (2′F-ANA)-History, properties and new frontiers. *Can. J. Chem.*, **86**, 641–656.
23. Watts,J.K., Katolik,A., Viladoms,J. and Damha,M.J. (2009) Studies on the hydrolytic stability of 2′-fluoroarabinonucleic acid (2′F-ANA). *Org. Biomol. Chem.*, **7**, 1904–1910.
24. Martin-Pintado,N., Deleavey,G.F., Portella,G., Campos-Olivas,R., Orozco,M., Damha,M.J. and González,C. (2013) Backbone FC-H···O hydrogen bonds in 2′F-substituted nucleic acids. *Angew. Chem. Int. Ed.*, **52**, 12065–12068.
25. Morrissey,D., Blanchard,K., Shaw,L., Jensen,K., Lockridge,J., Dickinson,B., McSwiggen,J., Vargeese,C., Bowman,K., Shaffer,C. *et al.* (2005) Activity of stabilized short interfering RNA in a mouse model of hepatitis B virus replication. *Hepatology*, **41**, 1349–1356.
26. de Fougerolles,A., Vornlocher,H.P., Maraganore,J. and Lieberman,J. (2007) Interfering with disease: a progress report on siRNA-based therapeutics. *Nature Rev. Drug Discov.*, **6**, 443–453.
27. Terrazas,M., Alagia,A., Faustino,I., Orozco,M. and Eritja,R. (2013) Functionalization of the 3′-ends of DNA and RNA strands with N-ethyl-N coupled nucleosides: A promising approach to avoid 3′-exonuclease-catalyzed hydrolysis of therapeutic oligonucleotides. *ChemBioChem*, **14**, 510–520.
28. Abe,N., Abe,H. and Ito,Y. (2007) Dumbbell-shaped nanocircular RNAs for RNA interference. *J. Am. Chem. Soc.*, **129**, 15108–15109.
29. Wei,L., Cao,L. and Xi,Z. (2013) Highly potent and stable capped siRNAs with picomolar activity for RNA interference. *Angew. Chem. Int. Ed.*, **52**, 6501–6503.
30. Hamasaki,T., Suzuki,H., Shirohzu,H., Matsumoto,T., D'Alessandro-Gabazza,C.N., Gil-Bernabe,P., Boveda-Ruiz,D., Naito,M., Kobayashi,T., Toda,M. *et al.* (2012) Efficacy of a novel class of RNA interference therapeutic agents. *PLoS One*, **7**, e42655.
31. Han,D.C., Shen,T.-L. and Guan,J.-L. (2001) The Grb7 family proteins: structure, interaction with other signaling molecules and potential cellular functions. *Oncogene*, **20**, 6315–6327.
32. Beaucage,S. and Caruthers,M. (1981) Deoxynucleoside phosphoramidites - a new class of key intermediates for deoxypolynucleotide synthesis. *Tetrahedron Lett.*, **22**, 1859–1862.
33. Frisch,M.J., Trucks,G.W., Schlegel,H.B., Scuseria,G.E., Robb,M.A., Cheeseman,J.R., Scalmani,G., Barone,V., Mennucci,B. and Petersson,G.A. (2009) *Gaussian 09, revision A. 02*. Gaussian, Inc., Wallingford, Vol. **19**, pp. 227–238.
34. Wang,J., Cieplak,P. and Kollman,P.A. (2000) How well does a restrained electrostatic potential (RESP) model perform in calculating conformational energies of organic and biological molecules? *J. Comput. Chem.*, **21**, 1049–1074.
35. Case,D.A., Babin,V., Berryman,J., Betz,R.M., Cai,Q., Cerutti,D.S., Cheatham,T.E., Darden,T.A., Duke,R.E., Gohlke,H. *et al.* (2014) *AMBER 14*, University of California, San Francisco.
36. Ivani,I., Dans,P.D., Noy,A., Pérez,A., Faustino,I., Hospital,A., Walther,J., Andrio,P., Goñi,R., Balaceanu,A. *et al.* (2016) Parmbsc1: a refined force field for DNA simulations. *Nat. Methods*, **13**, 55–58.
37. Jorgensen,W.L., Chandrasekhar,J., Madura,J.D., Impey,R.W. and Klein,M.L. (1983) Comparison of simple potential functions for simulating liquid water. *J. Chem. Phys.*, **79**, 926–935.
38. Smith,D.E. and Dang,L.X. (1994) Computer simulations of NaCl association in polarizable water. *J. Chem. Phys.*, **100**, 3757–3766.
39. Lavery,R., Moakher,M., Maddocks,J.H., Petkeviciute,D. and Zakrzewska,K. (2009) Conformational analysis of nucleic acids revisited: Curves+. *Nucleic Acids Res.*, **37**, 5917–5929.
40. Noronha,A.M., Noll,D.M., Wilds,C.J. and Miller,P.S. (2002) $N^4$C-Ethyl-$N^4$C cross-linked DNA: Synthesis and characterization of duplexes with interstrand cross-links of different orientations. *Biochemistry*, **41**, 760–771.
41. Uhler,S., Cai,D., Man,Y., Figge,C. and Walter,N.G.J. (2003) RNA degradation in cell extracts: real-time monitoring by Fluorescence Resonance Energy Transfer. *J. Am. Chem. Soc.*, **125**, 14230–14231.
42. MacRae,I.J., Li,F., Zhou,K., Cande,W.Z. and Doudna,J.A. (2006) *Structure of Dicer and mechanistic implicatios for RNAi. Cold Spring Harbor Symposia on Quantitative Biology*, Cold Spring Harbor Laboratory Press, NY, Vol. **LXXI**, pp. 73–80.
43. Hutvágner,G. and Zamore,P.D. (2002) A microRNA in a multiple-turnover RNAi enzyme complex. *Science*, **297**, 2056–2060.
44. Zhang,H., Kolb,F.A., Brondani,V., Billy,E. and Filipowicz,W. (2002) Human Dicer preferentially cleaves dsRNAs at their termini without requirement of ATP. *EMBO J.*, **21**, 5875–5885.
45. Pradip,D., Bouzyk,M., Dey,N. and Leyland-Jones,B. (2013) Dissecting GRB7-mediated signals for proliferation and migration in HER2 overexpressing HER2 breast tumor cells: GTP-ase rules. *Am. J. Cancer Res.*, **3**, 173–195.
46. Bai,T. and Luoh,S.-W. (2007) GRB-7 facilitates HER2/Neu-mediated signal transduction and tumor formation. *Carcinogenesis*, **29**, 473–479.
47. Nencioni,A., Cea,M., Garuti,A., Passalacqua,M., Raffaghello,L., Soncini,D., Zoppoli,G., Pistoia,V., Patrone,F. and Ballestrero,A. (2010) Grb7 upregulation is a molecular adaptation to HER2 signaling inhibition due to removal of Akt-mediated gene repression. *PLoS One*, **5**, e9024.
48. Ramsey,B., Bai,T., Newel,A.H., Troxell,M., Park,B., Olson,S., Keenan,E. and Luoh,S.-W. (2011) GRB7 protein over-expression and clinical outcome in breast cancer. *Breast Cancer Res. Treat.*, **127**, 659–669.
49. Kao,J. and Pollack,J.R. (2006) RNA interference-based functional dissection of the 17q12 amplicon in breast cancer reveals contribution of coamplified genes. *Genes Chromosomes Cancer*, **45**, 761–769.
50. Starega-Roslan,J., Galka-Marciniak,P. and Krzyzosiak,W.J. (2015) Nucleotide sequence of miRNA precursor contributes to cleavage site selection by Dicer. *Nucleic Acids Res.*, **43**, 10939–10951.
51. Collingwood,M.A., Rose,S.D., Huang,L., Hillier,C., Amarzguioui,M., Wiiger,M.T., Soifer,H.S., Rossi,J.J. and Behlke,M.A. (2008) Chemical modification patterns compatible with high potency Dicer-substrate small interfering RNAs. *Oligonucleotides*, **18**, 187–200.